REDUCTION OF THE GRATING LOBES IN SPARSE ARRAY HOLOGRAPHIC SONAR BY PROJECTION ONTO CONVEX SETS

Kenbu Teramoto† *and Hikaru Kamiirisa*‡

† Department of Information Science, Faculty of Engineering,
Saga University, Saga, 840 JAPAN
‡ Akishima Laboratories (Mitsui Zosen) INC.

ABSTRACT

This paper describes a newly proposed image reconstruction algorithm and experimental results of a 3-D acoustical holographic imaging system which has an array composed of sparsely distributed transducer elements. The new algorithm is based on the projection onto convex sets (POCS) method. The POCS method allows the addition of convex sets constrained by the *a priori* information to reduce ambiguity in the image reconstruction process.

By several experiments, it is proved that the concept of the image reconstruction algorithm has following improvements:

1. the artifacts caused by the grating lobes can be reduced under the condition the interval length is much larger than the wave length,
2. the storage of the entire inverse matrix of K the degradation matrix of the imaging system is not required because the new image reconstruction algorithm is based on the localized projection procedures.
3. the instability to the noise caused by the lack of the knowledge of the point spread function can be reduced.

1. INTRODUCTION

An acoustic holography technique has been widely used in under-water visualization system, medical imaging system and NDT applications. In usual case, the signals are received by spatial arrays of transducers which are densely distributed and the images of the reflectivity in the object field can be reconstructed by the synthetic aperture technique. The interspacing of elements of the array is taken to be shorter than λ at the center frequency, because of reducing the interference of the grating lobes.

This work is supported by Akishima Laboratories (Mitsui Zosen) INC.

On the other hand, in the case that the transducer array is composed of a few number of elements and the interspacing is larger than λ, the reconstructed image is interfered by widely spread strong grating lobes and side lobes. Under such condition, in order to reconstruct an image of the characteristics of reflectivity of the object field, it is important to solve the following Fredholm integral equation all over the object field,

$$g(\boldsymbol{r}'') = \int_V h(\boldsymbol{r}, \boldsymbol{r}'') f(\boldsymbol{r}) \mathrm{d}\boldsymbol{r} + n(\boldsymbol{r}''). \qquad (1)$$

The discrete formulation can be written as

$$\boldsymbol{g} = H\boldsymbol{f} + \boldsymbol{n}, \qquad (2)$$

where $\boldsymbol{g}$, $\boldsymbol{f}$ and $\boldsymbol{n}$ are the lexicographic row-stacked vectors of discretized version of g,f,n in (1), respectively. H is the transfer matrix. However, in solving the above equation, the larger the considering volume window should be in order to improve the accuracy of the reflectivity estimates and statistical stability, the longer the computational time becomes.

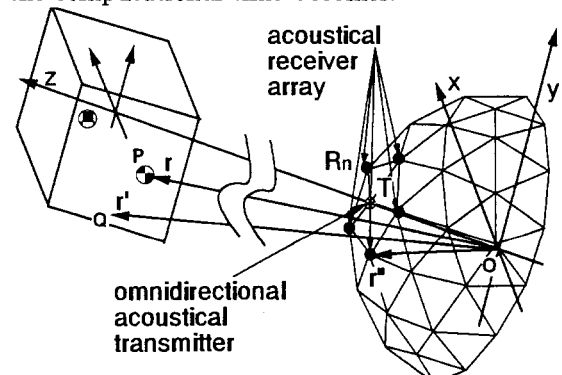

Fig.1 A geometrical view of an acoustical imaging system with sparse transducer array

2. PROBLEM FORMULATION

The considered acoustic holographic imaging system of interest is illustrated in Fig.1. Usually the holographic

0-7803-2431-5/95 $4.00

imaging system has two steps in the image reconstruction process. In the first step, the probing wave illuminates the object field and the scattered wave field is observed by the array composed of sparsely distributed transducer elements. In the second step, the image is formed by launching a conversing wave from the dipole sources applied on the same location of each element as illustrated in Fig.2. The second process is called back-propagation and denoted as

$$\boldsymbol{f}_b = H^T\boldsymbol{g} = H^TH\boldsymbol{f} + H^T\boldsymbol{n} = K\boldsymbol{f} + H^T\boldsymbol{n}, \quad (3)$$

where $K = H^TH$ is the back-propagation kernel matrix composed of the PSF of the imaging system. All signals received at the transducers from the point P suffers a total time delay Δt after processing. The signals from all the transducer elements are added so that the total amplitude N times the amplitude is the signal arriving at one element. However, it is possible for a point Q, located anywhere on the surface of a spheroid whose centers are R_n and T, to produce a signal with same delay time Δt. Hence the target on the above spheroid can give rise to spurious near-in and far-out grating lobes. The greater the number of the target in the object field becomes, the larger the affects generated by the spurious grating lobes. Near the focusing point, these surfaces overlap and there are phase additions and subtractions, yielding the typical PSF response like $(\sin(||\boldsymbol{r} - \boldsymbol{r}'||))/||\boldsymbol{r} - \boldsymbol{r}'||$. Farther out from the forcusing point, the spheroids only partially overlap or never overlap. Thus the grating lobe response cannot be washed out perfectly[2]. In order to reduce the power of grating lobes, it is necessary to introduce the least mean square solution given by

$$\hat{\boldsymbol{f}} = K^+\boldsymbol{f}_b = K^+H^T\boldsymbol{g}, \quad (4)$$

where K^+ denotes the psuedo - inverse of K. But the size of the matrix K and K^+ is too large, it is difficult to require the storage of the entire $K+$ from the point of practical view.

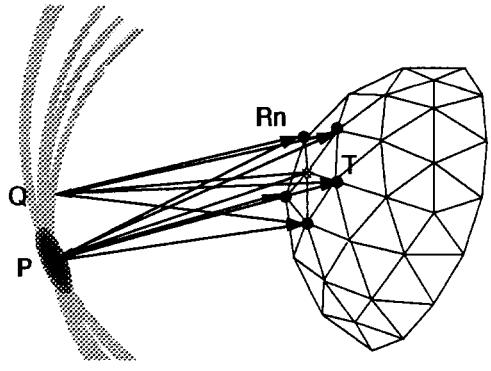

Fig.2Causes of near-in and far-out grating lobes

3. IMAGE RECONSTRUCTION ALGORITHM

The images can be reconstructed by Kaczmarz algorithm as following equation[1]:

$$\begin{aligned}\boldsymbol{f}^{[k+1]} &= \boldsymbol{f}^{[k]} + ((H^TH)^+H^T)\Lambda(\boldsymbol{g} - H\boldsymbol{f}^{[k]}) \\ &= (I - \Lambda)\boldsymbol{f}^{[k]} + \Lambda(K^+f_b + (I - K^+K)\boldsymbol{f}^{[k]}). \quad (5)\end{aligned}$$

The newly proposed image reconstruction algorithm uses approximated inverse matrix$\hat{K}^-$ in the place of the pseudo inverse of K and *a priori* information. Each raw of $\hat{K}^-$ is composed of the inverse filter which satisfies the admissible condition of the PSF near in the each focusing point. Under the least square constraint as:

$$||\boldsymbol{g} - H\tilde{\boldsymbol{f}}||^2 \rightarrow \text{minimum}, \quad (6)$$

the updating equation of the iterative image reconstruction can be denoted as:

$$\tilde{\boldsymbol{f}}^{[k+1]} = (I - \Lambda)\tilde{\boldsymbol{f}}^{[k]} + \Lambda(\hat{K}^-\boldsymbol{f}_b + (I - \hat{K}^-\hat{K})\tilde{\boldsymbol{f}}^{[k]}). \quad (7)$$

In addition to the least square constraint (6), *a priori* knowledge is used in the proposed image reconstruction process utilizing POCS method. Let us suppose that the knowledges are associated with L sets. Since the desired reconstructed image satisfies all of the constraints, it should be in the intersection set C_0 as:

$$\boldsymbol{f} \in C_R = \bigcap_{l=0}^{L-1} C_l. \quad (8)$$

Let P_i be orthogonal projection operator onto the set C_i defined as:

$$||\boldsymbol{f} - \tilde{\boldsymbol{f}}|| = \inf_{a \in C_R} ||\boldsymbol{f} - \boldsymbol{a}||. \quad (9)$$

The POCS method can be expressed as following successive projection onto the convex sets:

$$\boldsymbol{f}^{[k+1]} = (I - \Lambda)\boldsymbol{f}^{[k]} + \Lambda P_l(\boldsymbol{f}^{[k]}), \quad (10)$$

where λ_k denotes the relaxation parameter[1].

In the The proposed iterative image reconstruction algorithm is shown as following several steps.

[step0] The estimate $\tilde{\boldsymbol{f}}^{[0]}$ is initialized :

$$\begin{aligned}&k = 0; \\ &\tilde{\boldsymbol{f}}^{[k]} = \boldsymbol{f}_b = H^T\boldsymbol{g};\end{aligned}$$

[step1] $\tilde{\boldsymbol{f}}^{[k]}$ is updated under the least square constraint:

$$\tilde{\boldsymbol{f}}^{[k+1]} = (I - \Lambda)\tilde{\boldsymbol{f}}^{[k]} + \Lambda(\hat{K}^+\boldsymbol{f}_b + (I - \hat{K}^+\hat{K})\tilde{\boldsymbol{f}}^{[k]});$$

[step2] The projection of the estimate $\tilde{f}^{[k]}$ onto the lth closed convex set

for $l = 1$ **to** L **do**
$\tilde{f}^{[k+1]} = (I - \Lambda_l)f^{[k]} + \Lambda P_l(f^{[k]})$;
$k = k + 1$;

[step3]

$\forall\ i\ |\tilde{f}_i^{[k]} - \tilde{f}_i^{[k-L]}|^2 < \mathrm{EPS}$
then END
else go to [step1];

4. EXPERIMENTAL RESULTS

To verify the proposed image reconstruction algorithm, we have implemented and tested the newly proposed algorithm and the regularized direct inversion through numerical experiments. The direct inversion with regularization method gives as:

$$\tilde{f} = (\hat{K} + \lambda I)^{-1} H^T g \qquad (11)$$

where the value of λ is the Lagrangian constant.

4.1. PARTIALLY KNOWN POINT SPREAD FUNCTION

The image of the point scatterer obtained by back propagation is shown in Fig.3.1. which is the original PSF of the sparse array holographic sonar. Near the location of the scatterer, the image has the typical PSF response like Farther out from the point, the grating lobe response has pentagonally symmetric characteristic. In the image reconstruction process, the partially known PSF shown in Fig.3.2. is used for $\hat{K}^-$. The filter for selecting pentagonally symmetric pattern is used in the proposed image reconstruction process.

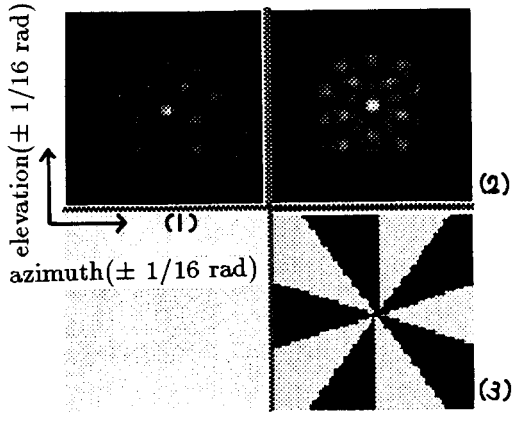

Fig.3 Transversal distribution of (1): original PSF of the conventional holographic method, (2): example of partially(quater area of original PSF) known PSF and (3): Filter for selecting pentagonally symmetric pattern.

4.2. BASIC IMAGING PERFORMANCE

The image obtained by the conventional back propagation is shown in Fig.4.1. The image reconstructed by regularized direct inversion method with $\hat{K}^-$ is shown in Fig.4.2. This image is disturbed by the unstability caused by the pentagonally symmetric grating lobes that is $K - \hat{K}$. The image reconstructed by the proposed algorithm is shown in Fig.4.3. The following constraints are applied in the image reconstruction process:

- the reflectivity ranges between -1.0 to $+1.0$,
- the PSF has pentagonally symmetric characteristic.
- the reflectivity of the object field is distributed smoothly.

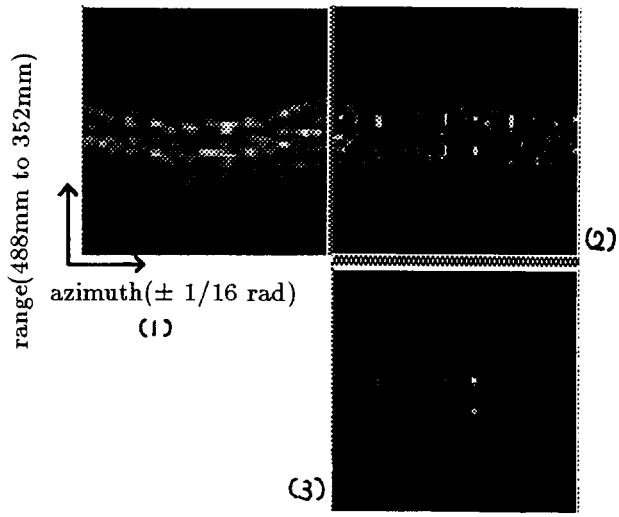

Fig.4 Longitudinal distributions of reconstructed images of 4-point scatterers located 400±10 ahead and separated by $2\pi/64$ (rad) in the elevational direction obtained (1): by conventional back propagation, (2): by direct inversion and (3): by the proposed reconstruction algorithm with partially known PSF.

4.3. STABILITY ANALYSIS

In the experiments, the stability of the above two image reconstruction algorithms are evaluated under the following conditions, [A1]:original PSF is known, [A2]:0.5 x0.5 area of original PSF is known, [A3]:0.38x0.38 area of original PSF is known, [A4]:0.25x0.25 area of original PSF is known and the various input noise levels :[B1]input S/N=96dB, [B2]input S/N=48dB, [B3]input S/N=24dB. [B4]input S/N=12dB, [B5]input S/N=6dB. Under the each condition, the RMS residual error of the proposed image reconstruction process based on POCS

and that of the regularized dilect inversion method are plotted in the Fig.5. The images reconstructed by regularized direct inversion method with $\hat{K}^-$ are shown in Fig.6. and those reconstructed by the proposed algorithm are shown in Fig.7.

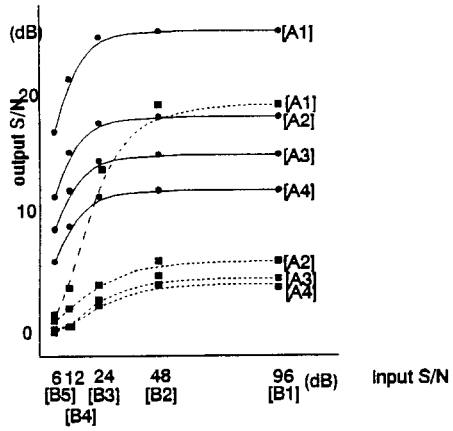

Fig.5 Signal to noise ratio of the reconstructed images when independent additive noise at each receiving element exists. Dashed curves with solid squares obtained by direct inversion method under the following conditions [A1]:original PSF is known, [A2]:0.5x0.5 area of original PSF is known, [A3]:0.38x0.38 area of original PSF is known, [A4]:0.25x0.25 area of original PSF is known. Solid curves with solid circles obtained by the proposed image reconstruction algorithm utilizing *a priori*information under the same conditions.

5. CONCLUDING REMARKS

The image reconstruction algorithm is proposed with practical advantages. This new algorithm dose not require the complete back-propagation kernel matrix K and its inverse matrix K^- due to the use of local projection procedures and additional *a priori*information. In addition, the artifacts caused by the grating robes can be reduced under the condition the interval length is much larger than the wave length and the accuracy of the reflectivity estimates and statistical stability can be improved compared to the reconstructed images by the regularized direct inversion algorithm.

REFERENCES

[1] R.J.Mammone, "Computational Methods of Signal Recovery and Recognition," Wiley, 1992

[2] G.S.Kino, "Acoustic Waves, Devices, Imaging and Analog Signal Processing," Prentice-Hall, pp.229-243, 1988

[3] Y. Tamura, et al., "Holographic Sonar Using Orthogonal Transmitting Pulses", Acoustical Imaging, 17, pp.753-760, 1989

[4] S.Kuo, R.J.Mammone,"Resolution enhancement of tomographic images using the row action projection method", IEEE Trans. Med. Imaging, vol.10-4, pp.593-601, 1991

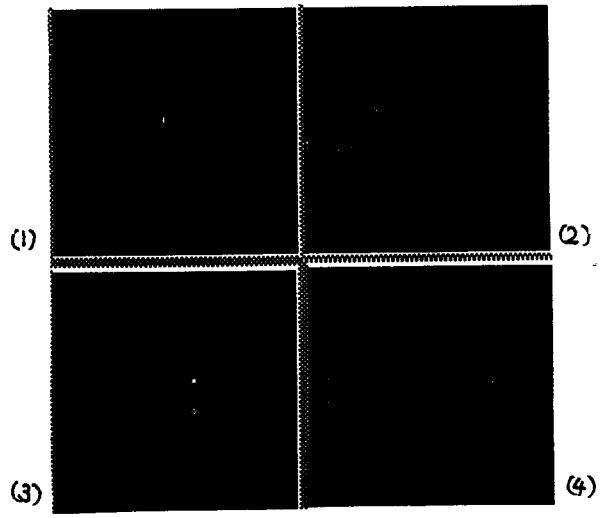

Fig.6 Longitudinal distributions of reconstructed images of 4 point-scatterers reconstructed by direct inversion method when independent additive noise at each receiving element exists under the following conditions (1): [A2][B2], (2): [A4][B2], (3): [A2][B5], (4): [A4][B5].

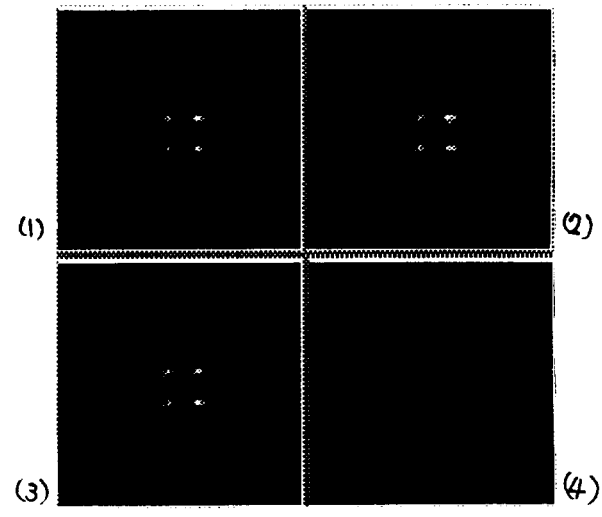

Fig.7 Longitudinal distributions of reconstructed images of 4 point-scatterers reconstructed by proposed method utilizing *a priori*information when independent additive noise at each receiving element exists under the following conditions (1): [A2][B2], (2): [A4][B2], (3): [A2][B5], (4): [A4][B5].